

Radiative decay $Z_H \rightarrow \gamma A_H$ in the little Higgs model with T-parity

I. Cortés-Maldonado and G. Tavares-Velasco

*Facultad de Ciencias Físico Matemáticas, Benemérita Universidad Autónoma de Puebla,
Apartado Postal 1152, Puebla, Pue., México*

In the little Higgs model with T-parity (LHTM), the only tree-level kinematically allowed two-body decay of the Z_H boson can be the $Z_H \rightarrow A_H H$ decay and thus one-loop induced two-body decays may have a significant rate. We study the $Z_H \rightarrow \gamma A_H$ decay, which is induced at the one-loop level by a fermion triangle and is interesting as it depends on the mechanism of anomaly cancellation of the model. All the relevant two- and three-body decays of the Z_H gauge boson arising at the tree-level are also calculated. We considered a small region of the parameter space where f is still allowed to be as low as 500 GeV by electroweak precision data. We analyzed the scenario of a Higgs with a mass of 120 GeV. We found that the $Z_H \rightarrow \gamma A_H$ branching ratio can be of the order of a tree-level three-body decay and may be at the reach of detection at the LHC for f close to 500 GeV, but it may be difficult to detect for $f = 1$ TeV. There is also an scenario where the Higgs boson has an intermediate mass such that the $Z_H \rightarrow A_H H$ decay is closed, the $Z_H \rightarrow \gamma A_H$ gets considerably enhanced and the chances of detection get a large boost.

PACS number(s):14.70.Pw,13.38.Dg

1. Introduction

Little Higgs models offer a solution to the little hierarchy problem based on the idea that the Higgs boson is a pseudo-Goldstone boson arising from an approximately broken global symmetry associated with a strongly interacting sector. Although some models based on this idea were already proposed long ago,^{1,2} they were unsuccessful as there was the need to reintroduce fine-tuning to obtain a light Higgs boson. A solution to this problem was proposed in Ref. 3: by invoking a collective mechanism of symmetry breaking, the gauge and Yukawa couplings of the Goldstone boson are introduced in such a way that the Higgs boson mass is free of quadratic divergences at the one-loop or even at the two-loop level. Several realizations of this idea have been proposed in the literature, but the most popular is the littlest Higgs model (LHM).⁴ Apart from reproducing the SM at the electroweak scale, the LHM predicts heavy partners for the SM gauge bosons and the top quark, which are necessary to cancel the quadratic divergences of the Higgs boson mass at the one-loop level. However, this model predicts large corrections to electroweak precision observables and the scale of the global symmetry breaking, f , is constrained by experimental data to be larger than about 4000 GeV.⁵ One alternative to evade this strong constraint relies on the introduction of a discrete symmetry called T-parity,⁶ which forbids any dangerous contributions to electroweak observables and allows

for much weaker constraints on f .⁷ The littlest Higgs model with T parity (LHTM) has become the source of considerable interest in the literature recently.^{8,9,10}

The LHTM is a nonlinear sigma model that has a global symmetry under the group $SU(5)$ and a local symmetry under the subgroup $[SU(2) \times U(1)]^2$. There is two extra neutral gauge bosons, Z_H and A_H , that are the partners of the Z gauge boson and the photon, respectively. While the Z_H gauge boson is associated with the extra $SU(2)$ gauge group, the photon partner is associated with the extra $U(1)$ gauge group. The latter particle is the lightest one of the model and is a promising dark matter candidate. It is not possible to obtain a model-independent bound on the mass of an extra neutral gauge boson from experimental measurements, but electroweak precision data¹¹ (EWPD) along with Tevatron¹² and LEP2¹³ searches, allow one to obtain limits on its mass from about 500 GeV to 1000 GeV in models with universal flavor gauge couplings. While an extra neutral gauge boson with a mass around 1 TeV may be detected at the LHC, the future international linear collider would be able to produce it with a mass up to 2-5 TeV.¹⁴ This would open up potential opportunities to study the phenomenology of this particle.

In the LHTM, the new gauge bosons are T-odd and the SM particles are T-even. Therefore T-parity invariance imposes severe restrictions on the decay modes of the new particles. While the heavy photon is stable, the only tree-level kinematically allowed two body-decay of the Z_H gauge boson is $Z_H \rightarrow A_H H$. We are interested in studying the one-loop induced decay $Z_H \rightarrow \gamma A_H$, which may have a significant branching ratio similar to that of a tree-level three-body decay. This decay is interesting as its signature at particle colliders would be very peculiar. In addition, the respective decay width could be useful to explore the mechanism of anomaly cancellation present in the model. Decays of an extra neutral gauge boson into a pair of neutral gauge bosons have already been studied in the literature, for instance in the context of a superstring-inspired E_6 model,¹⁵ the minimal 331 model,¹⁶ 5D warped-space models,¹⁷ and little Higgs model without T-parity.¹⁸ The remainder of this paper is structured as follows. In Section II we present a survey of the LHTM, with particular emphasis on the gauge sector and the properties of the extra neutral gauge boson Z_H . Section III is devoted to present the calculation of the one-loop decay $Z_H \rightarrow \gamma A_H$. We will also discuss the dominant decay modes of the Z_H boson arising at the tree-level. Section IV is devoted to discuss the results, and the conclusions are presented in Sec. V.

2. The framework of the little Higgs model with T-parity

In the LHM, the largest corrections to electroweak precision observables arise from the heavy gauge bosons.⁵ A global fit to experimental data yields a strong constraint on the symmetry breaking scale, $f > 4$ TeV, for a wide region of the space of parameters.⁵ This would require reintroducing fine-tuning to have a light Higgs boson. Once T-parity is introduced into the model,⁶ the tree-level contributions to electroweak observables arising from the heavy gauge bosons cancel, and the

resulting constraints on the scale f are significantly weaker: there is an area in the parameter space where f is allowed to be as low as 500 GeV,⁷ which depends on the Higgs boson mass value and the ratio between the masses of the T-odd and T-even top partners.

2.1. The scalar and gauge sectors

The LHM is a nonlinear sigma model with a global symmetry under the $SU(5)$ group and a gauged subgroup $[SU(2) \otimes U(1)]^2$. The Goldstone bosons are parametrized by the following Σ field

$$\Sigma = e^{i\Pi/f} \Sigma_0 e^{i\Pi^T/f}, \quad (1)$$

where Π is the pion matrix. The Σ field transforms under the gauge group as $\Sigma \rightarrow \Sigma' = U \Sigma U^T$, with $U = L_1 Y_1 L_2 Y_2$ an element of the gauge group.

The $SU(5)$ global symmetry is broken down to $SO(5)$ by the sigma field VEV, Σ_0 , which is of the order of the scale of the symmetry breaking. After the global symmetry is broken, 14 Goldstone bosons arise accommodated in multiplets of the electroweak gauge group: a real singlet, a real triplet, a complex triplet and a complex doublet. The latter will be identified with the SM Higgs doublet. At this stage, the gauge symmetry is also broken to its diagonal subgroup, $SU(2) \times U(1)$. The real singlet and the real triplet are absorbed by the gauge bosons associated with the broken gauge symmetry.

The LHM effective Lagrangian is assembled by the kinetic energy Lagrangian of the Σ field, \mathcal{L}_K , the Yukawa Lagrangian, \mathcal{L}_Y , and the kinetic terms of the gauge and fermion sectors. The sigma field kinetic Lagrangian is given by⁴

$$\mathcal{L}_K = \frac{f^2}{8} \text{Tr} |D_\mu \Sigma|^2, \quad (2)$$

with the $[SU(2) \times U(1)]^2$ covariant derivative defined by⁴

$$D_\mu \Sigma = \partial_\mu \Sigma - i \sum_{j=1}^2 [g_j W_{j\mu}^a (Q_j^a \Sigma + \Sigma Q_j^{aT}) + g'_j B_{j\mu} (Y_j \Sigma + \Sigma Y_j^T)]. \quad (3)$$

The heavy $SU(2)$ and $U(1)$ gauge bosons are $W_j^\mu = \sum_{a=1}^3 W_j^{\mu a} Q_j^a$ and $B_j^\mu = B_j^\mu Y_j$, with Q_j^a and Y_j the gauge generators, while g_i and g'_i are the respective gauge couplings. The VEV Σ_0 generates masses for the gauge bosons and mixing between them. The heavy gauge boson mass eigenstates are given by⁴

$$W'^a = -c W_1^a + s W_2^a, \quad (4)$$

$$B' = -c' B_1 + s' B_2, \quad (5)$$

with masses $m_{W'} = \frac{f}{2} \sqrt{g_1^2 + g_2^2}$ and $m_{B'} = \frac{f}{\sqrt{20}} \sqrt{g_1'^2 + g_2'^2}$.

The orthogonal combinations of gauge bosons are identified with the SM gauge bosons:⁴

$$W^a = s W_1^a + c W_2^a, \quad (6)$$

$$B = s' B_1 + c' B_2, \quad (7)$$

which remain massless at this stage, their couplings being given by $g = g_1 s = g_2 c$ and $g' = g'_1 s' = g'_2 c'$, where $s = g_2/\sqrt{g_1^2 + g_2^2}$ and $s' = g'_2/\sqrt{g_1'^2 + g_2'^2}$ are mixing parameters.

The gauge and Yukawa interactions that break the global $SO(5)$ symmetry induce radiatively a Coleman-Weinberg potential, V_{CW} , whose explicit form can be obtained after expanding the Σ field:

$$V_{CW} = \lambda_{\phi^2} f^2 \text{Tr}|\phi|^2 + i\lambda_{h\phi h} f (h\phi^\dagger h^T - h^* \phi h^\dagger) - \mu^2 |h|^2 + \lambda_{h^4} |h|^4, \quad (8)$$

where λ_{ϕ^2} , $\lambda_{h\phi h}$, and λ_{h^4} depend on the fundamental parameters of the model, whereas μ^2 , which receives logarithmic divergent contributions at one-loop level and quadratically divergent contributions at the two-loop level, is treated as a free parameter of the order of $f^2/16\pi^2$. The Coleman-Weinberg potential induces a mass term for the complex triplet Φ , whose components acquire masses of the order of f . The neutral component of the complex doublet develops a VEV, v , of the order of the electroweak scale, which is responsible for EWSB. The VEV v along with the triplet VEV, v' , are obtained when V_{CW} is minimized.

In the gauge sector, T-parity only exchanges the $[SU(2) \times U(1)]_1$ and $[SU(2) \times U(1)]_2$ gauge bosons: $W_1^{\mu a} \leftrightarrow W_2^{\mu a}$ and $B_1^\mu \leftrightarrow B_2^\mu$. T-parity invariance is achieved by setting the coupling constants at the values $g_1 = g_2$ and $g'_1 = g'_2$.⁶ The light SM gauge bosons are T-even, while the heavy gauge bosons are T-odd. At the electroweak scale, EWSB proceeds as usual, yielding the final mass eigenstates: the three SM gauge bosons are accompanied by three heavy gauge bosons which are their counterpart, A_H , W_H and Z_H . The masses of the heavy gauge bosons get corrected by terms of the order of $(v/f)^2$ and so are the masses of the weak gauge bosons W_L and Z_L . The heavy gauge boson masses are given by:

$$m_{Z_H} \simeq m_{W_H} = gf \left(1 - \frac{v^2}{8f^2} \right), \quad (9)$$

$$m_{A_H} = \frac{g'f}{\sqrt{5}} \left(1 - \frac{5v^2}{8f^2} \right). \quad (10)$$

As far as the scalar sector of the theory is concerned, due to the transformation property of the Σ field under T-parity ($\Sigma \rightarrow \bar{\Sigma} = \Sigma_0 \Omega \Sigma^\dagger \Omega \Sigma_0$, with $\Omega = \text{diag}(1, 1, -1, 1, 1)$) the SM Higgs doublet turns out to be T-even, while the additional $SU(2)_L$ triplet Φ is T-odd. The $H\Phi H$ coupling is thus forbidden and so is a nonzero $SU(2)_L$ triplet VEV, v' . After diagonalizing the Higgs mass matrix, the light Higgs boson mass can be obtained at the leading order

$$m_H^2 = 2\mu^2 = 2 \left(\lambda_{h^4} - \frac{\lambda_{h\phi h}^2}{\lambda_{\phi^2}} \right) v^2 \quad (11)$$

It is required that $\lambda_{h^4} > \lambda_{h\phi h}^2/\lambda_{\phi^2}$ to obtain the correct electroweak symmetry breaking vacuum with $m_H^2 > 0$. The Higgs triplet masses are degenerate at this order: $m_\Phi = \sqrt{2}m_H f/v$.

In summary, in the gauge and scalar sectors both the LHM and the LHTM have the same particle content.⁶ T-parity invariance has important phenomenological consequences as there are only vertices containing an even number of T-odd particles. The heavy photon, which is the lightest new particle, is stable and thus a dark matter candidate. The Z_H gauge boson can only decay into a kinematically allowed odd number of heavy photons accompanied by SM particles.

2.2. Fermion sector

In order to avoid compositeness constraints,⁶ T-parity requires two $SU(2)$ doublets, q_1 and q_2 , for each SM doublet. Under a T-parity transformation, these doublets are exchanged $q_1 \leftrightarrow -q_2$. The T-even (T-odd) combination of q_1 and q_2 is the SM (T-odd) fermion doublet. The mass of each T-odd fermion doublet is generated by the interaction

$$\mathcal{L}_\kappa = -\kappa_f (\bar{\Psi}_2 \xi \Psi_c + \bar{\Psi}_1 \Omega \xi^\dagger \Omega \Psi_c), \quad (12)$$

where the $SU(5)$ multiplets Ψ_i are defined by $\Psi_1 = (q_1, 0, \mathbf{0}_2)^T$ and $\Psi_2 = (\mathbf{0}_2, 0, q_2)^T$, with $q_{1,2} = -\sigma_2(u_{1,2L}, d_{1,2L})^T$. Also, the multiplet $\Psi_c = (q_c, \chi_c, \tilde{q}_c)^T$ is introduced such that it transforms nonlinearly under $SU(5)$. It can be shown that \mathcal{L}_κ is T-parity invariant as the following transformation rules are obeyed: $\Psi_{1,2} \rightarrow -\Sigma_0 \Psi_{2,1}$, $\Psi_c \rightarrow -\Psi_c$, $\xi \rightarrow \Omega \xi^\dagger \Omega$, and $\Sigma \rightarrow \Sigma_0 \Omega \Sigma^\dagger \Omega \Sigma_0$.

It is easy to see that the components of the T-odd doublet $q_- = (q_1 + q_2)/\sqrt{2} = (id_{-L}, -iu_{-L})^T$ have the following masses

$$m_{u_-} \sim \sqrt{2} \kappa f \left(1 - \frac{v^2}{8f^2} \right), \quad (13)$$

$$m_{d_-} = \sqrt{2} \kappa f. \quad (14)$$

The effects of the heavy T-odd fermions has been investigated in Ref. 9 and it was shown that they may be non-negligible at high-energy colliders. For simplicity, an universal value for κ will be assumed for all the T-odd fermions. Also, flavor nondiagonal interactions will be neglected.

In order to cancel the quadratic divergences to the Higgs boson mass arising from the SM top quark, the top sector must be additionally modified. The corresponding $SU(5)$ multiplets are completed by introducing two $SU(2)$ singlets U_{1L} and U_{2L} : $Q_1 = (q_1, U_{1L}, \mathbf{0}_2)^T$ and $Q_2 = (\mathbf{0}_2, U_{2L}, q_2)^T$. The T-parity invariant Yukawa Lagrangian for the top sector can be written as

$$\begin{aligned} \mathcal{L}_t^Y = & \frac{\lambda_1 f}{2\sqrt{2}} \epsilon_{ijk} \epsilon_{xy} \left((\bar{Q}_1)_i \Sigma_{jx} \Sigma_{ky} - (\bar{Q}_2 \Sigma_0)_i \tilde{\Sigma}_{jx} \tilde{\Sigma}_{ky} \right) u_{+R} \\ & - \lambda_2 f (\bar{U}_{1L} U_{1R} + \bar{U}_{2L} U_{2R}) + \text{H.c.}, \end{aligned} \quad (15)$$

From here we can obtain the mass eigenstates: there are a new T-odd quark $T_- = (U_{1L} + U_{2R})/\sqrt{2}$ and a new T-even quark T_+ . The latter together with the top quark are given by:

$$\begin{pmatrix} u_{+X} \\ U_{+X} \end{pmatrix} = \begin{pmatrix} c_X & s_X \\ -s_X & c_X \end{pmatrix} \begin{pmatrix} t_{+X} \\ T_{+X} \end{pmatrix}, \quad (16)$$

for $X = L, R$ and with the T-even eigenstates defined as $u_+ = (u_1 - u_2)/\sqrt{2}$. The mixing angles are $s_L \sim s_\alpha^2 v/f$ and $s_R \sim s_\alpha = \lambda_1/\sqrt{\lambda_1^2 + \lambda_2^2}$. The masses of the new T-odd and T-even quarks are given to the lowest order by⁸:

$$m_{T_+} = \sqrt{\lambda_1^2 + \lambda_2^2} f, \quad (17)$$

$$m_{T_-} = \lambda_2 f, \quad (18)$$

with the top mass given by

$$m_t = \frac{\lambda_1 \lambda_2}{\sqrt{\lambda_1^2 + \lambda_2^2}} v, \quad (19)$$

The above Yukawa interaction also corrects the SM couplings with terms of the order of $(v/f)^2$.

In summary, each SM fermion has associated a T-odd fermion with a mass given by Eq. (14) and there is a new T-even top partner T_+ that has its associated T-odd fermion T_- . The interactions of the T-even fermions and their T-odd partners with the neutral gauge bosons are given by:⁹

$$\mathcal{L} = \sum_{u,d} \bar{f}_L \gamma^\mu f_{-L} ((g_{c_H} T_{3f} + g' c_H Y') Z_{H\mu} + (-g_{s_H} T_{3f} + g' c_H Y') A_{H\mu}) + \text{H.c.} \quad (20)$$

where $Y' = -1/10$, $s_H \simeq gg'/(g^2 - g'^2/5)v^2/(4f^2)$ describes the degree of mixing between neutral heavy gauge bosons, and $c_H^2 = 1 - s_H^2$. s_H . The corresponding Feynman rules are shown in Appendix B along with those for the couplings of the Z gauge boson to T-odd fermions and also the interaction vertices for the heavy gauge bosons.

3. One-loop decay $Z_H \rightarrow \gamma A_H$

Because of T-parity invariance, the Z_H gauge boson can only decay into one heavy photon plus other SM particles, although the decay into three heavy photons can also be kinematically allowed. As long as the Higgs boson mass is light, the only kinematically allowed Z_H tree-level two-body decay is $Z_H \rightarrow A_H H$. The respective decay width can be written as

$$\begin{aligned} \Gamma(Z_H \rightarrow A_H H) &= \frac{g_{Z_H A_H H}^2}{192\pi m_{Z_H} y_{A_H}} \sqrt{(1 - (\sqrt{y_H} - \sqrt{y_{A_H}})^2)(1 - (\sqrt{y_H} + \sqrt{y_{A_H}})^2)} \\ &\times (1 + (y_H - y_{A_H})^2 + y_Z^2 - 2(y_H - 5y_{A_H})). \end{aligned} \quad (21)$$

where $g_{Z_H A_H H} = gg'v/2$ and $y_a = (m_a/m_{Z_H})^2$. The following three-body decays are also allowed: $Z_H \rightarrow A_H WW$, $Z_H \rightarrow A_H ZZ$, $Z_H \rightarrow A_H \bar{f}f$, and even $Z_H \rightarrow A_H HH$ and $Z_H \rightarrow 3A_H$. To obtain the respective decay widths, we squared the decay amplitude with the aid of the FeynCalc package¹⁹ and the integration over the three-body phase space was performed numerically via the internal Mathematica routines. We refrain from presenting the analytical results as they are too cumbersome to be included here.

At the one-loop level the decay $Z_H \rightarrow \gamma A_H$ proceeds through a fermion triangle and its amplitude depends on the mechanism of anomaly cancellation. We expect that the branching ratio for this decay can compete with those of the tree-level three-body decays, which are suppressed due to phase-space. The decay $Z_H \rightarrow \gamma A_H$ proceeds via the Feynman diagram of Fig. 1, which involves two fermions of opposite T-parity circulating in the loop.

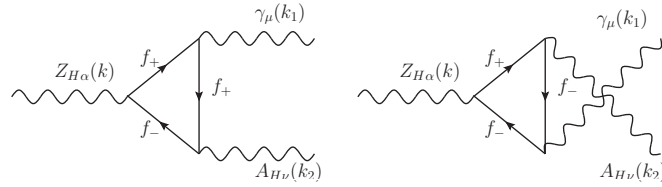


Fig. 1. One-loop Feynman diagrams contributing to the Z_H gauge boson decay $Z_H \rightarrow \gamma A_H$ in the LHTM. f_+ stands for a T-even charged fermion and f_- for its associated T-odd charged fermion.

The decay amplitude for the $Z_H \rightarrow \gamma A_H$ decay can be written as

$$\begin{aligned} \mathcal{M}(Z_H \rightarrow \gamma A_H) = & \frac{1}{m_{Z_H}^2} \epsilon_\alpha(k) \epsilon_\mu(k_1) \epsilon_\nu(k_2) \left\{ iA_1^{\gamma A_H} (k_1^\nu \epsilon^{\alpha\mu\lambda\rho} + k_1^\alpha \epsilon^{\mu\nu\lambda\rho}) k_{1\lambda} k_{2\rho} \right. \\ & + iA_2^{\gamma A_H} k_1 \cdot k_2 \epsilon^{\alpha\mu\nu\lambda} k_{1\lambda} + A_3^{\gamma A_H} k_1^\alpha (k_1 \cdot k_2 g^{\mu\nu} - k_1^\nu k_2^\mu) \\ & \left. + A_4^{\gamma A_H} k_1^\nu (k_1 \cdot k_2 g^{\alpha\mu} - k_1^\alpha k_2^\mu) \right\}, \end{aligned} \quad (22)$$

which was arranged in this peculiar form to display electromagnetic gauge invariance. Here k_1^μ and k_2^ν are the 4-momenta of the outgoing γ and A_H gauge bosons, whereas k^α is the 4-momentum of the Z_H gauge boson. The mass-shell and transversality conditions, along with Schouten's identity, were used to eliminate redundant terms. The explicit form of the $A_i^{\gamma A_H}$ coefficients is shown in Appendix A in terms of Passarino-Veltman scalar functions. Once the $Z_H \rightarrow \gamma A_H$ amplitude is squared and summed (averaged) over polarizations of the ingoing (outgoing) gauge bosons, the decay width can be written as

$$\begin{aligned} \Gamma(Z_H \rightarrow \gamma A_H) = & \frac{1}{3} \frac{(1 - y_{A_H})^5 (1 + y_{A_H}) m_{Z_H}}{2^5 \pi y_{A_H}} \left(|A_1^{\gamma A_H} - A_2^{\gamma A_H}|^2 + |A_3^{\gamma A_H}|^2 \right. \\ & \left. + |A_4^{\gamma A_H}|^2 \right). \end{aligned} \quad (23)$$

We will evaluate the $Z_H \rightarrow \gamma A_H$ branching ratio for values of the parameters consistent with the constraints from EWPD.

4. Numerical results and discussion

4.1. Current constraints on the LHTM parameter space

Before presenting our results we would like to discuss on the current constraints on the parameter space of the LHTM from EWPD. In Ref. 7, the symmetry breaking scale f was constrained via the oblique parameters S , T and U , together with the $Z \rightarrow \bar{b}b$ decay. A similar analysis was done more recently in Ref. 20. It was found that the allowed values of the scale f depend on the Higgs boson mass and the ratio of the masses of the T-odd and T-even top partners, $s_\lambda = m_{T_-}/m_{T_+}$. The contribution to the T parameter from the each T-odd fermion doublet was found to be ⁷

$$T_{\text{T-odd}} = -\frac{\kappa^2}{192\pi^2\alpha} \left(\frac{v}{f}\right)^2, \quad (24)$$

Thus the contribution from the T-odd fermions is negligible as long as they are relatively light, but it can be significant if they are too heavy. Along these lines, an upper bound on the T-odd fermion masses can be found from the LEP bound on four-fermion interactions: ⁷

$$m_{f_-} < 4.8 \left(\frac{f}{1 \text{ TeV}}\right)^2 \text{ TeV}. \quad (25)$$

This leads to a maximal contribution to the T parameter of about 0.05 for each T-odd fermion as long as its mass reaches this upper bound.⁷ If such a maximal contribution is taken into account, the allowed area on the f vs m_H plane shrinks considerably, although f below 1 TeV is still allowed for some values of s_λ and m_H .²⁰

As far as the direct search of T-odd quarks is concerned, the D0 Collaboration has obtained a lower bound on the T-odd quark mass from the search for final events with jets and large missing transverse energy at the Tevatron.²¹ According to this bound, which depends on the mass of the heavy photon m_{A_H} , a light T-odd quark with a mass of about 100 GeV is not ruled out by Tevatron data as long as $m_{A_H} \simeq 100$ GeV. More recently, the search for final events with jets and large missing transverse energy at the LHC has been used by the CMS²² and Atlas²³ Collaborations to search for supersymmetry. An analysis presented in Ref. 24 shows that the LHC data can also be used to impose a bound on the T-odd quark masses that is stronger than the one found at the Tevatron. It was concluded that m_{q_-} below 450 GeV is ruled out for $m_{A_H} \simeq 100$ GeV with 95 % C.L. Furthermore, the data collected at the LHC during the years 2011 and 2012 will be useful to place a bound on the T-quark mass of about 650 GeV for the $m_{A_H} \simeq 300$ GeV and below.^{citePerelstein:2011ds}

We will see below that the possible detection of the $Z_H \rightarrow \gamma A_H$ decay at the LHC would be very difficult for f above 1 TeV as the estimated production of $pp \rightarrow W_H Z_H$ events would require a branching ratio above the 0.1 level to have just a handful of $Z_H \rightarrow \gamma A_H$ events. We thus must seek for regions of the parameter space where f is still allowed to be below 1 TeV. From the results presented in Ref. 20 for the allowed area on the f vs m_H plane with 95 % C.L., we can conclude that there are two promising scenarios for observing the $Z_H \rightarrow \gamma A_H$ decay channel at the LHC: one scenario in which the T-odd fermions are relatively light and another scenario in which they are very heavy. We will illustrate these scenarios assuming particular values for the parameters s_λ and κ . The first scenario to be analyzed corresponds to $s_\lambda = 0.55$ and the presence of T-odd fermions heavy enough to give a large contribution to the T parameter. This scenario would allow for values of f as low as about 600 GeV for a wide range of values of m_H . Another potential scenario arises when $s_\lambda = 0.75$ and the T-odd fermions are light enough to allow one to neglect their contribution to the T parameter, thereby allowing a large region of the parameter space. To accomplish these two scenarios we can choose convenient values of the parameter κ to tune the mass of the T-odd fermions. For instance, we show in Fig. 2 the contribution to the T parameter from a T-odd fermion when $\kappa = 0.7$ and $\kappa = 1.7$. We conclude that when $\kappa = 1.7$, the contribution from a T-odd fermion to the T parameter is close to the maximal value only for small f , but when $\kappa = 0.7$, the contribution from a T-odd fermion is about one order of magnitude below. In the latter case we will assume that these kind of contributions to the T parameter can be neglected.

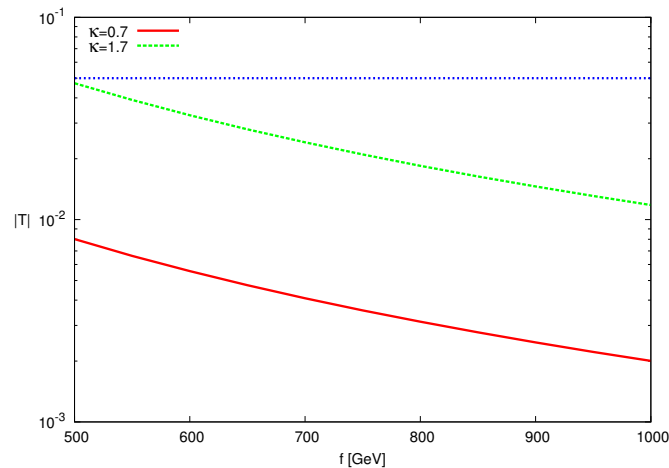


Fig. 2. Contribution of each T-odd fermion doublet to the oblique parameter T for two values of κ . The horizontal line is the maximal contribution from a T-odd fermion assuming that its mass reaches the the upper bound from the LEP bound on four fermion contact interactions.

4.2. Scenario with heavy T -odd fermions

According to the above discussion, we will consider the following values for the LHTM parameters: $m_H = 120$ GeV, $s_\lambda = 0.55$, and $\kappa = 1.7$. In Fig. 3 we show the branching ratio for the $Z_H \rightarrow \gamma A_H$ decay together with those of the relevant tree-level decays as functions of the scale of the symmetry breaking. The LoopTools package^{25,26} was used to evaluate the Passarino-Veltman scalar functions required by the $Z_H \rightarrow \gamma A_H$ decay width. In this scenario, the dominant decay mode is $Z_H \rightarrow A_H H$, which has a branching ratio of about 100% for $f \simeq 500$ GeV and about 80% for $f \simeq 2$ TeV. Other kinematically allowed tree-level decays, such as $Z_H \rightarrow A_H H H$, $Z_H \rightarrow A_H W W$, $Z_H \rightarrow A_H Z Z$, $Z_H \rightarrow A_H \bar{t} t$ and $Z_H \rightarrow A_H A_H A_H$, have branching ratios of the order of 1% for $f \simeq 500$ GeV, which increase as f increases. In particular, the $Z_H \rightarrow A_H W W$ branching ratio increases up to 10% for $f \simeq 2$ TeV. Although decays into a heavy photon plus a pair of light fermions are also kinematically allowed, their decay width is negligibly as the main contribution arises from a Feynman diagram where the fermion pair is emitted off the Higgs boson. We also observe that the branching ratio for the decay into three heavy photons can be of similar size than the ones for other three-body decays in the region of low f but it decreases quickly as f increases. This decay proceeds as follows: for f below about 465 GeV, the m_{A_H} is below 60 GeV and thus the Z_H gauge boson decays into a heavy photon plus a real Higgs boson with a mass of 120 GeV, which subsequently decays into a heavy photon pair. For $f > 465$ GeV, $m_{A_H} > m_H/2$, so the intermediate Higgs boson is virtual. As for the one-loop decay $Z_H \rightarrow \gamma A_H$, the respective branching ratio is of the order of less than one percent for $f = 500$ GeV, but it increases slightly for $f = 2$ TeV. We would like to note that the Z_H branching ratios are not very sensitive to a change in the value of the s_λ parameter.

An interesting scenario arises when the Higgs boson has an intermediate mass such that $m_H > Z_H - A_H$. In this case the $Z_H \rightarrow A_H H$ decay channel will be closed and the $Z_H \rightarrow \gamma A_H$ decay has a substantial enhancement. This situation occurs, for instance, for m_H about 300 GeV and f up to 600 GeV or either for m_H about 500 GeV and f up to 1 TeV. Such scenarios are still allowed by EWPD for some particular values of s_λ . We have calculated the branching ratios of the main Z_H decays for $m_H = 300$ GeV, $s_\lambda = 0.55$ and $\kappa = 1.7$. We show the results in Fig. 4. The dominant decay mode is now $Z_H \rightarrow A_H W W$, whereas the $Z_H \rightarrow \gamma A_H$ decay width is even larger than the one for the $Z_H \rightarrow A_H Z Z$ decay. In general, $BR(Z_H \rightarrow \gamma A_H)$ gets enhanced up to two orders of magnitude with respect to what is obtained in the scenario with a light Higgs boson. When $f \simeq 600$ GeV, $BR(Z_H \rightarrow \gamma A_H)$ drops suddenly as the threshold for the opening of the $Z_H \rightarrow A_H H$ decay is reached.

4.3. Scenario with relatively light T -odd fermions

We now consider the case of $m_H = 120$ GeV, $s_\lambda = 0.75$ and $\kappa = 0.7$. This means that the T -odd fermions are relatively light and their contribution to the T parameter

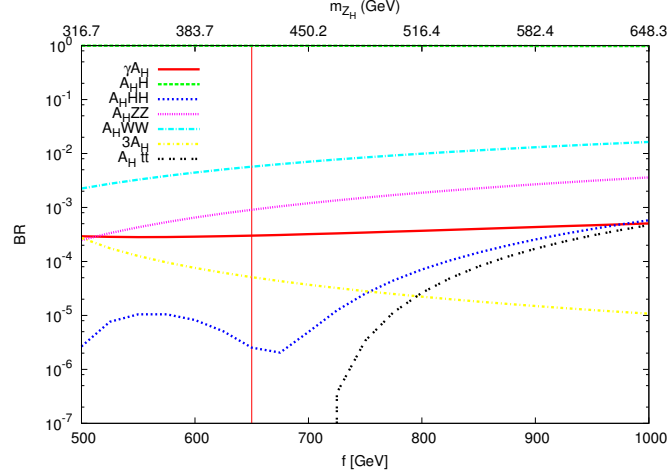


Fig. 3. Branching ratio for the one-loop decay $Z_H \rightarrow \gamma A_H$ in the LHTM as a function of the scale of symmetry breaking f . We also include the main tree-level two- and three-body decays. We used $m_H = 120$ GeV, $s_\lambda = 0.55$, and $\kappa = 1.7$. The region to the right of the vertical line is not allowed by EWPD.

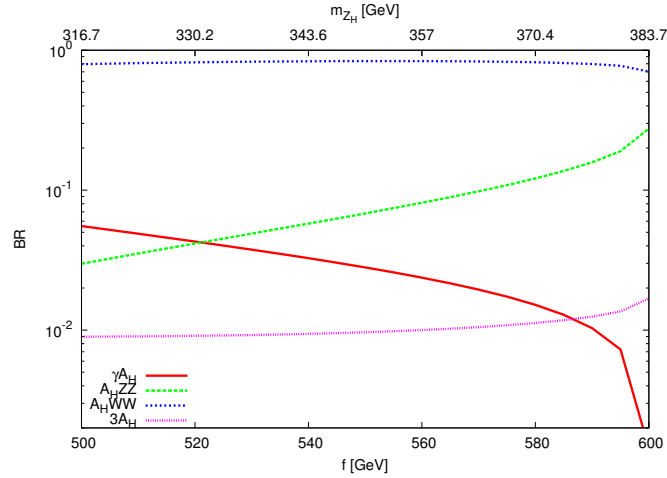


Fig. 4. The same as in Fig. 3, but for $m_H = 300$ GeV.

is small. We show in Fig. 5 the relevant Z_H branching ratios for this scenario. We observe that the $Z_H \rightarrow \gamma A_H$ branching ratio is enhanced by about one order of magnitude with respect to the scenario with heavy T-odd fermions. Even more, the $Z_H \rightarrow \gamma A_H$ branching ratio can be as large as the $Z_H \rightarrow A_H WW$ branching ratio for small f , but the latter increases steadily with f and it becomes much larger for f close to 1 TeV. Overall the $Z_H \rightarrow \gamma A_H$ branching ratio is of the same order of magnitude as the one for the $Z_H \rightarrow A_H ZZ$ decay over a large range of f . We also

would like to consider the case of an intermediate Higgs boson. We show in Fig. 6 the Z_H branching ratios for $s_\lambda = 0.75$, $\kappa = 0.7$, and $m_H = 300$ GeV. The situation looks similar to that depicted in Fig. 4. The branching ratio for the $Z_H \rightarrow \gamma A_H$ decay shows a large increase and it is the subdominant Z_H decay channel for up to $f \simeq 570$ GeV, where it starts to decrease quickly. Although the $Z_H \rightarrow \gamma A_H$ decay can have a substantial enhancement over a wide f range if the Higgs boson is heavier, the Z_H production cross section decreases quickly as f increases, so the $Z_H \rightarrow \gamma A_H$ decay would be more difficult to detect for f close to 1 TeV.

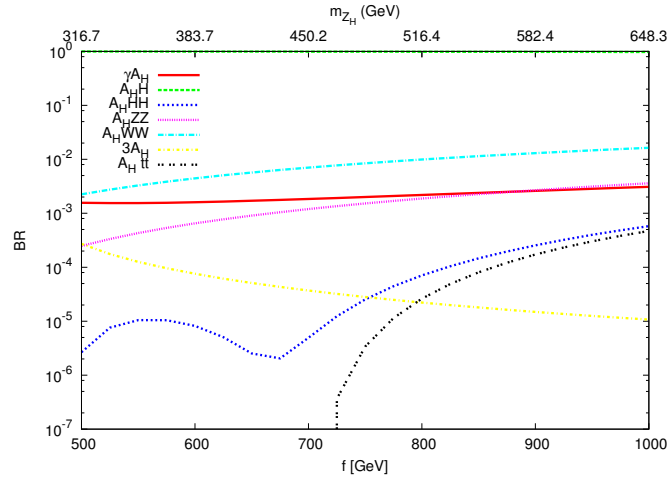


Fig. 5. The same as in Fig. 3, but for $s_\lambda = 0.75$, and $\kappa = 0.7$.

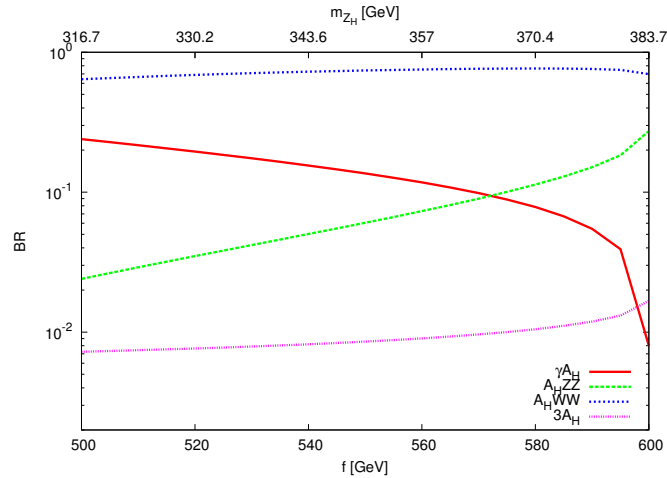


Fig. 6. The same as in Fig. 5, but for $m_H = 300$ GeV.

4.4. Experimental prospects at the LHC

At the LHC, the T-odd gauge bosons must be pair produced due to T-parity invariance. The dominant Z_H production mode is $pp \rightarrow W_H Z_H$, whereas other production modes such as $pp \rightarrow Z_H Z_H$ and $pp \rightarrow A_H Z_H$ are suppressed by more than one and two orders of magnitude, respectively. We show in Fig. 7 the dominant Z_H production mode at the LHC for the two scenarios described above and $\sqrt{s} = 14$ TeV. The CTEQ6M PDF set was used.²⁸ This calculation was obtained via the CalcHep package²⁷ along with the LHTM files provided by the authors of Ref. 9. In Fig. 7 we also observe that a luminosity of 300 fb^{-1} would allow for a large number of $pp \rightarrow W_H Z_H$ events, of the order of 10^5 for $f = 500$ GeV and 10^2 for $f = 2$ TeV.

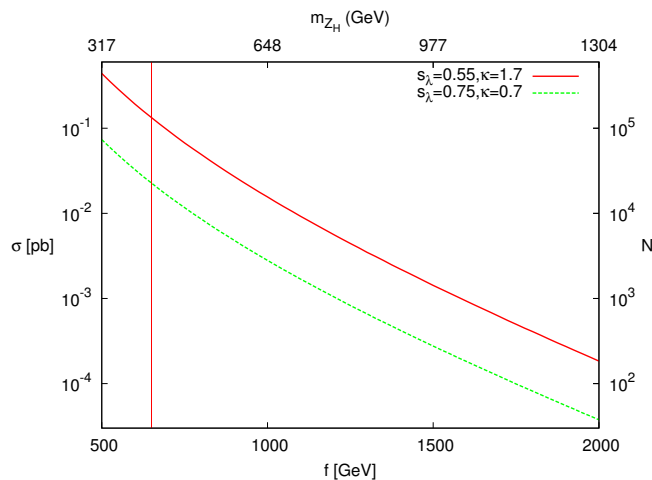


Fig. 7. Cross section for $pp \rightarrow W_H Z_H$ at the LHC in the two scenarios described in the text. In this plot $\sqrt{s} = 14$ TeV and the CTEQ6M PDF set was used. The expected number of events is shown in the left axis for a luminosity of 300 fb^{-1} . The region to the right of the vertical line is not allowed for $s_\lambda = 0.55$ by EWPD.

Assuming that the W_H gauge boson decays as $W_H \rightarrow A_H W$ with a rate of 100%, we have calculated the expected number of $pp \rightarrow W_H Z_H \rightarrow W A_H + \gamma A_H$ events for a luminosity of 300 fb^{-1} . For the scenarios discussed above, the dependence on the scale of the symmetry breaking of the expected number of $pp \rightarrow W_H Z_H \rightarrow W A_H + \gamma A_H$ events is shown in Fig. 8 (light Higgs boson) and Fig. 9 (intermediate Higgs boson). In the case of a light Higgs boson, we observe that the event number is of the order of one hundred around $f = 500$ GeV and decreases quickly as f increases. As far as the scenario with an intermediate Higgs boson is concerned, there would be a large number of events for $f = 500$ GeV, but a sharp decrease is observed for f about 600 GeV, where the $Z_H \rightarrow A_H H$ channel gets opened.

The experimental signature of the $Z_H \rightarrow \gamma A_H$ decay would be a charged lepton accompanied by an energetic photon plus large missing transverse energy \cancel{E}_T . The

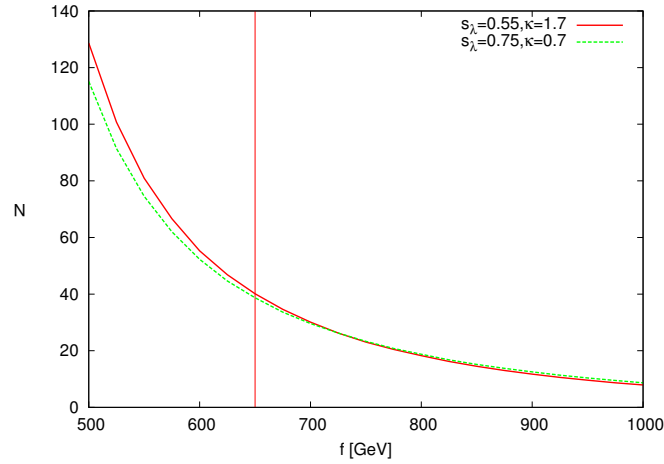


Fig. 8. Expected number of $pp \rightarrow W_H Z_H \rightarrow A_H W + \gamma A_H$ events at the LHC for $\sqrt{s} = 14$ TeV in the scenario with a light Higgs boson with a mass $m_H = 120$ GeV. A luminosity of 300 fb^{-1} was considered. The region to the right of the vertical line is not allowed for $s_\lambda = 0.55$ by EWPD.

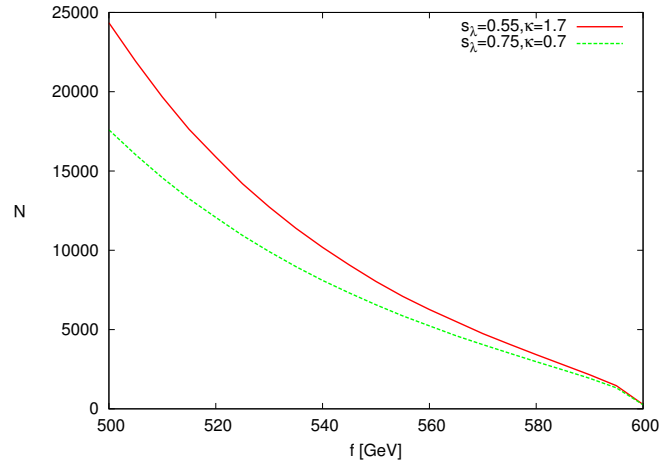


Fig. 9. The same as in Fig. 8, but for $m_H = 300$ GeV.

main background comes from the SM process $pp \rightarrow W\gamma \rightarrow \ell\nu\gamma$, but it can be largely reduced by imposing cuts on the photon energy. In the scenario with a light Higgs boson, the $Z_H \rightarrow \gamma A_H$ detection seems promising, but a more detailed Monte Carlo analysis would be required to make further conclusions. As for the scenario with an intermediate Higgs boson is concerned, although there is a large number of $W A_H + \gamma A_H$ events for $f \simeq 500$ GeV, it drops drastically for $f \simeq 600$ GeV, which would make the $Z_H \rightarrow \gamma A_H$ decay detection very difficult for large f .

5. Final remarks

We have examined the one-loop decay $Z_H \rightarrow \gamma A_H$ in the framework of the LHTM. Since T-parity restricts the number of possible decay channels of the heavy Z_H gauge boson, one-loop Z_H decays can have branching fractions of similar order of magnitude as some Z_H tree-level three-body decays. One advantage of the $Z_H \rightarrow \gamma A_H$ decay channel is that it would not require the previous detection of the Higgs boson. We have examined two potential scenarios still allowed by EWPD: relatively light or heavy T-odd fermions. In the case of a light Higgs boson, with a mass of 120 GeV, the expected number of $pp \rightarrow W_H Z_H \rightarrow A_H W + \gamma A_H$ events is of the order of one hundred for $f \simeq 500$ GeV, but it decreases quickly for increasing f . The possible detection of the $Z_H \rightarrow \gamma A_H$ decay looks thus only favorable for f about 500 GeV. Other Z_H production modes, such as $pp \rightarrow A_H Z_H$ and $pp \rightarrow Z_H Z_H$, would give less than 10 $Z_H \rightarrow \gamma A_H$ events for $f \simeq 500$ GeV and would not be useful to detect this decay mode. An interesting scenario is that in which there is an intermediate Higgs boson with a mass of the order of 300 GeV. From 500 GeV to 600 GeV, the $Z_H \rightarrow A_H H$ is closed and the event number of $pp \rightarrow W_H Z_H \rightarrow A_H W + \gamma A_H$ events gets enhanced by more than three orders of magnitude with respect to the case of a light Higgs boson. This scenario would be more favorable for the detection of the $Z_H \rightarrow \gamma A_H$ decay but also requires that f is not too large to allow the opening of the $Z_H \rightarrow A_H H$ channel.

Acknowledgments

GTV acknowledge support from Conacyt and SNI (México). We also acknowledge support from VIEP-BUAP.

Appendix A. Form factors for the $Z_H \rightarrow \gamma A_H$ decay

In this appendix we present the explicit form for the $A_i^{\gamma A_H}$ coefficients in terms of Passarino-Veltman scalar functions. They are given as follows:

$$\begin{aligned}
A_1^{\gamma A_H} = & \left(\frac{g}{8\pi c_W} \right)^2 \frac{2}{(1 - y_{A_H})^3 y_{A_H}} \sum_{f_{\pm}} \xi_{\gamma A_H}^f \left\{ y_{A_H}^3 \left[2 + B_{c_{\pm}} - B_{a_{\pm}} \right. \right. \\
& + 2((2y_{f_{\pm}} + 1)C_{a_{\mp}} - y_{f_{\mp}}(C_{a_{\mp}} - C_{a_{\pm}})) \Big] \\
& + y_{A_H}^2 \left[(y_{f_{\pm}} - y_{f_{\mp}})(3B_{c_{\pm}} - 2B_{a_{\pm}} - B_{a_{\mp}}) - 2(1 + 3(B_{b_{\pm}} - B_{c_{\pm}})) \right. \\
& \left. - 2(2y_{f_{\mp}} C_{a_{\pm}} + (1 - (y_{f_{\pm}} - y_{f_{\mp}})^2)C_{a_{\mp}}) \right] \\
& + y_{A_H} \left[2(y_{f_{\pm}} - y_{f_{\mp}})(2B_{c_{\pm}} + B_{a_{\pm}} - 3B_{b_{\pm}}) + B_{a_{\pm}} - B_{c_{\pm}} \right. \\
& \left. - 2(((y_{f_{\pm}} - y_{f_{\mp}})^2 + 2y_{f_{\pm}} - y_{f_{\mp}})C_{a_{\mp}} - y_{f_{\mp}} C_{a_{\pm}}) \right] \\
& \left. + (y_{f_{\pm}} - y_{f_{\mp}})(B_{a_{\pm}} - B_{c_{\pm}}) \right\}, \tag{A.1}
\end{aligned}$$

$$\begin{aligned}
A_2^{\gamma A_H} = & \left(\frac{g}{8\pi c_W} \right)^2 \frac{2}{(1-y_{A_H})^3 y_{A_H}} \sum_{f_+} \left\{ \xi_{\gamma A_H}^f \left[y_{A_H}^3 (B_{a_+} - B_{c_{\pm}} \right. \right. \\
& - 2(1 + (y_{f_+} - y_{f_-} + 1)C_{a_{\mp}})) + y_{A_H}^2 ((y_{f_+} - y_{f_-})(2B_{a_+} + B_{a_{\pm}} - 3B_{c_{\pm}}) \\
& + 2(1 + B_{b_{\pm}} - B_{c_{\pm}}) + 2(2y_{f_-}C_{a_{\pm}} - (y_{f_+} - y_{f_-})^2 C_{a_{\mp}} + C_{a_{\pm}})) \\
& + y_{A_H} (B_{c_{\pm}} - B_{a_+} + 2(y_{f_+} - y_{f_-})((3B_{b_{\pm}} - 2B_{c_{\pm}} - B_{a_+}) \\
& + (y_{f_+} - y_{f_-} + 1)C_{a_{\mp}}) - 4y_{f_-}C_{a_{\pm}}) + (y_{f_+} - y_{f_-})(B_{c_{\pm}} - B_{a_{\pm}}) \left. \right] \\
& + 2\tilde{\lambda}_{\gamma A_H}^f (1 - y_{A_H})^2 \sqrt{y_{f_+}} \sqrt{y_{f_-}} (C_{a_{\pm}} + C_{a_{\mp}}) \left. \right\}, \tag{A.2}
\end{aligned}$$

$$\begin{aligned}
A_3^{\gamma A_H} = & \left(\frac{g}{8\pi c_W} \right)^2 \frac{2}{(1-y_{A_H})^3} \sum_{f_+} \left\{ \tilde{\xi}_{\gamma A_H}^f \left[2y_{A_H}^2 (y_{f_-}C_{a_{\pm}} - y_{f_+}C_{a_{\mp}}) \right. \right. \\
& + \frac{4}{3}y_{A_H} (y_{f_+}(2B_{a_+} + B_{a_{\pm}} - 3B_{c_{\pm}}) - y_{f_-}(2B_{a_-} + B_{a_{\pm}} - 3B_{c_{\pm}}) \\
& - (y_{f_+} - y_{f_-})(1 + 3(y_{f_-}C_{a_{\pm}} + y_{f_+}C_{a_{\mp}}))) \\
& + \frac{2}{3}(2y_{f_-}(B_{a_{\pm}} + 2B_{a_-} + 3B_{c_{\pm}} - 6B_{b_{\pm}} - 1) \\
& - 2y_{f_+}(2B_{a_+} + B_{a_{\pm}} + 3B_{c_{\pm}} - 6B_{b_{\pm}} - 1) \\
& + 6(y_{f_+} - y_{f_-})(y_{f_-}C_{a_{\pm}} - y_{f_+}C_{a_{\mp}}) + 3(y_{f_+}C_{a_{\mp}} - y_{f_-}C_{a_{\pm}}) \left. \right] \\
& + 2\tilde{\lambda}_{\gamma A_H}^f (1 - y_{A_H})^2 \sqrt{y_{f_+}} \sqrt{y_{f_-}} (C_{a_{\mp}} - C_{a_{\pm}}) \left. \right\}, \tag{A.3}
\end{aligned}$$

$$A_4^{\gamma A_H} = \frac{1}{y_{A_H}} A_3^{\gamma A_H} \left(y_{A_H} \leftrightarrow \frac{1}{y_{A_H}} \right), \tag{A.4}$$

where the scalar functions are as follows

$$B_{a_+} = B_0(0, m_{f_+}^2, m_{f_+}^2), \tag{A.5}$$

$$B_{a_{\pm}} = B_0(0, m_{f_+}^2, m_{f_-}^2), \tag{A.6}$$

$$B_{a_-} = B_0(0, m_{f_-}^2, m_{f_-}^2), \tag{A.7}$$

$$B_{b_{\pm}} = B_0(m_{Z_H}^2, m_{f_+}^2, m_{f_-}^2), \tag{A.8}$$

$$B_{c_{\pm}} = B_0(m_{A_H}^2, m_{f_+}^2, m_{f_-}^2), \tag{A.9}$$

$$C_{a_{\pm}} = m_{Z_H}^2 C_0(m_{A_H}^2, 0, m_{Z_H}^2, m_{f_+}^2, m_{f_-}^2, m_{f_-}^2), \tag{A.10}$$

$$C_{a_{\mp}} = m_{Z_H}^2 C_0(m_{A_H}^2, 0, m_{Z_H}^2, m_{f_-}^2, m_{f_+}^2, m_{f_+}^2). \tag{A.11}$$

Also

$$\xi_{\gamma A_H}^f = N_c^f Q^f \left(g_L^f g_L^{\prime\prime f} + g_R^f g_R^{\prime\prime f} \right), \quad (\text{A.12})$$

$$\tilde{\xi}_{\gamma A_H}^f = N_c^f Q^f \left(g_L^f g_L^{\prime\prime f} - g_R^f g_R^{\prime\prime f} \right), \quad (\text{A.13})$$

$$\lambda_{\gamma Z}^f = N_c^f Q^f \left(g_L^f g_R^{\prime\prime f} + g_R^f g_L^{\prime\prime f} \right), \quad (\text{A.14})$$

$$\tilde{\lambda}_{\gamma Z}^f = N_c^f Q^f \left(g_L^f g_R^{\prime\prime f} - g_R^f g_L^{\prime\prime f} \right), \quad (\text{A.15})$$

where $g_{L,R}^f$ ($g_{L,R}^{\prime\prime f}$) are the constants associated with the $Z_H \bar{f}_+ f_-$ ($A_H \bar{f}_+ f_-$) coupling (See Appendix A). The sum runs over each charged T-even fermion and its associated T-odd fermion. In the case of the top sector, the fermions to be summed are the pairs (t, t_-) , (t, T_-) , (T_+, t_-) , and (T_+, T_-) . Notice that $A_3^{\gamma A_H}$ and $A_4^{\gamma A_H}$ are antisymmetric under the exchange $f_+ \leftrightarrow f_-$, and thus vanish when the same fermion circulates into the loop. In addition, the transition amplitude vanishes when $y_{A_H} = 1$ as required for the on-shell $Z_H Z_H \gamma$ vertex.

Appendix B. Feynman rules for the Z_H and A_H gauge bosons in the LHTM

In this appendix we collect all the Feynman rules necessary for our calculation. They were taken from Refs. 9 and 29.

Appendix B.1. Couplings to T-even and T-odd fermions

We write the couplings of the extra neutral Z_H gauge boson to T-even and T-odd fermions in the form:

$$\mathcal{L} = -\frac{ig}{c_W} \bar{f}_+ \gamma_\mu \left(g_L^f P_L + g_R^f P_R \right) f_- Z_H^\mu, \quad (\text{B.1})$$

with $P_{L,R}$ the usual chirality projectors. A similar expression holds for the A_H gauge boson couplings with the replacement $g_{L,R}^f \rightarrow g_{L,R}^{\prime\prime f}$. The respective coupling constants are shown in Table 1.

Appendix B.2. Couplings involving two heavy gauge bosons

We also need Feynman rules for the couplings $Z_H A_H H$, $A_H A_H H$, and $Z_H A_H H H$. These vertices are involved in the tree-level decays of the Z_H gauge boson. The respective Feynman rules are shown in Table 2 together with the Feynman rules for the trilinear and quartic gauge boson couplings involved in our calculation. We have defined

$$F^{\mu\nu\rho}(k_1, k_2, k_3) = g^{\mu\nu}(k_1 - k_2)^\rho + g^{\nu\rho}(k_2 - k_3)^\mu + g^{\rho\mu}(k_3 - k_1)^\nu, \quad (\text{B.2})$$

where all particles are outgoing, and

$$G^{\mu\nu\rho\sigma} = 2g^{\mu\nu}g^{\rho\sigma} - g^{\mu\rho}g^{\nu\sigma} - g^{\mu\sigma}g^{\nu\rho}. \quad (\text{B.3})$$

Table 1. Couplings of the the heavy neutral gauge bosons to a T-even antifermion and a T-odd fermion in the LHTM. The second line is valid for all the down-type fermions, but the first line is valid for all up-type fermions other than those of the top sector. The mixing angle is $s_H \sim gg'v^2/(g^2 - g'^2/5)/(4f^2)$, with $c_H^2 = 1 - s_H^2$.

	$V = Z_H$		$V = A_H$	
	g_L^f	g_R^f	$g_L^{\prime f}$	$g_R^{\prime f}$
$V\bar{u}u_-$	$\frac{gc_H}{2} - \frac{g's_H}{10}$	0	$-\frac{gs_H}{2} - \frac{g'c_H}{10}$	0
$V\bar{d}d_-$	$-\frac{gc_H}{2} - \frac{g's_H}{10}$	0	$\frac{gs_H}{2} - \frac{g'c_H}{10}$	0
$V\bar{t}t_-$	$\left(\frac{gc_H}{2} - \frac{g's_H}{10}\right) c_L$	0	$\left(-\frac{gs_H}{2} - \frac{g'c_H}{10}\right) c_L$	0
$V\bar{t}T_-$	$-\frac{2g's_H}{5} s_L$	$-\frac{2g'c_H}{5} s_R$	$-\frac{2g'c_H}{5} s_L$	$-\frac{2g's_H}{5} s_R$
VT_+t_-	$\left(\frac{gc_H}{2} - \frac{g's_H}{10}\right) s_L$	0	$\left(-\frac{gs_H}{2} - \frac{g'c_H}{10}\right) s_L$	
VT_+T_-	$\frac{2g's_H}{5} c_L$	$\frac{2g'c_H}{5} c_R$	$\frac{2g'c_H}{5} c_L$	$\frac{2g's_H}{5} c_R$

Table 2. Feynman rules for the vertices involved in the calculation of the Z_H gauge boson decays in the LHTM.

Vertex	Feynman rule
$A_H^\mu A_H^\nu H$	$-i\frac{g'v^2}{2}g^{\mu\nu}$
$Z_H^\mu A_H^\nu H$	$-i\frac{gg'v}{2}g^{\mu\nu}$
$Z_H^\mu A_H^\nu HH$	$-i\frac{gg'}{2}g^{\mu\nu}$
$A_H^\mu(k_1)W_H^\nu(k_2)W^\rho(k_3)$	$i\frac{5g}{4(5-t_W^2)}\frac{v^2}{f^2}F^{\mu\nu\rho}(k_1, k_2, k_3)$
$Z_H^\mu(k_1)W_H^\nu(k_2)W^\rho(k_3)$	$igF^{\mu\nu\rho}(k_1, k_2, k_3)$
$W^\mu W^\nu Z_H^\rho A_H^\sigma$	$-i\frac{5g^2v^2}{4(5-t_W^2)f^2}G^{\mu\nu\rho\sigma}$

References

1. D. B. Kaplan and H. Georgi, Phys. Lett. B **136**, 183 (1984).
2. D. B. Kaplan, H. Georgi and S. Dimopoulos, Phys. Lett. B **136**, 187 (1984).
3. N. Arkani-Hamed, A. G. Cohen and H. Georgi, Phys. Lett. B **513**, 232 (2001) [arXiv:hep-ph/0105239].
4. N. Arkani-Hamed, A. G. Cohen, E. Katz and A. E. Nelson, JHEP **0207**, 034 (2002) [arXiv:hep-ph/0206021].
5. C. Csaki, J. Hubisz, G. D. Kribs, P. Meade and J. Terning, Phys. Rev. D **67**, 115002 (2003) [arXiv:hep-ph/0211124].
6. I. Low, JHEP **0410**, 067 (2004) [arXiv:hep-ph/0409025].
7. J. Hubisz, P. Meade, A. Noble and M. Perelstein, JHEP **0601**, 135 (2006) [arXiv:hep-ph/0506042].
8. J. Hubisz and P. Meade, Phys. Rev. D **71**, 035016 (2005) [arXiv:hep-ph/0411264].
9. A. Belyaev, C. R. Chen, K. Tobe and C. P. Yuan, Phys. Rev. D **74**, 115020 (2006) [arXiv:hep-ph/0609179].
10. A. Freitas and D. Wyler, JHEP **0611**, 061 (2006) [arXiv:hep-ph/0609103].
11. J. Erler and P. Langacker, Phys. Rev. Lett. **84**, 212 (2000) [arXiv:hep-ph/9910315].
12. [ALEPH Collaboration and DELPHI Collaboration and L3 Collaboration and], arXiv:hep-ex/0511027.
13. J. Alcaraz *et al.* [ALEPH Collaboration and DELPHI Collaboration and L3 Collaboration and], arXiv:hep-ex/0612034.
14. P. Langacker, Rev. Mod. Phys. **81**, 1199 (2009) [arXiv:0801.1345 [hep-ph]].
15. D. Chang, W. Y. Keung and S. C. Lee, Phys. Rev. D **38**, 850 (1988).

16. M. A. Perez, G. Tavares-Velasco and J. J. Toscano, Phys. Rev. D **69**, 115004 (2004) [arXiv:hep-ph/0402156].
17. M. Perelstein and Y. H. Qi, Phys. Rev. D **82**, 015004 (2010) [arXiv:1003.5725 [hep-ph]].
18. I. Cortes-Maldonado, A. Fernandez-Tellez and G. Tavares-Velasco, arXiv:1109.4390 [hep-ph].
19. R. Mertig, M. Bohm and A. Denner, Comput. Phys. Commun. **64**, 345 (1991).
20. M. Baak *et al.*, arXiv:1107.0975 [hep-ph].
21. V. M. Abazov *et al.* [D0 Collaboration], Phys. Lett. B **668**, 357 (2008) [arXiv:0808.0446 [hep-ex]].
22. V. Khachatryan *et al.* [CMS Collaboration], Phys. Lett. B **698**, 196 (2011) [arXiv:1101.1628 [hep-ex]].
23. J. B. G. da Costa *et al.* [Atlas Collaboration], Phys. Lett. B **701**, 186 (2011) [arXiv:1102.5290 [hep-ex]].
24. M. Perelstein and J. Shao, Phys. Lett. B **704**, 510 (2011) [arXiv:1103.3014 [hep-ph]].
25. G. J. van Oldenborgh and J. A. M. Vermaseren, Z. Phys. C **46**, 425 (1990).
26. T. Hahn, Nucl. Phys. Proc. Suppl. **89**, 231 (2000) [arXiv:hep-ph/0005029].
27. A. Pukhov, [hep-ph/0412191].
28. J. Pumplin, D. R. Stump, J. Huston, H. L. Lai, P. M. Nadolsky and W. K. Tung, JHEP **0207**, 012 (2002) [arXiv:hep-ph/0201195].
29. T. Han, H. E. Logan, B. McElrath and L. T. Wang, Phys. Rev. D **67**, 095004 (2003) [arXiv:hep-ph/0301040].